Comparative study on displacement measurement sensors for high-speed railroad bridge

Soojin Cho[1a], Junhwa Lee[2b] and Sung-Han Sim[*2]

[1]*Department of Civil Engineering, University of Seoul, Seoul 02504, South Korea*
[2]*School of Urban and Environmental Engineering, Ulsan National Institute of Science and Technology, Ulsan 44919, South Korea*

Abstract.   This paper presents a comparative study of displacement measurement using four sensors that are being used in the field: they are a ring gauge, a laser Doppler vibrometer (LDV), a vision-based displacement measurement system (VDMS), and an optoelectronic displacement meter (ODM). The comparative study was carried out on a brand-new high-speed railroad bridge designed to produce displacements within a couple of millimeters under the loading of a high-speed train. The tests were carried out on a single-span steel plate girder bridge two times with different train loadings: KTX and HEMU. The measured displacement is compared as raw and further discussion was made on the measurement noise, peak displacement, and frequency response of four sensors. The comparisonsare summarized to show the pros and cons of the used sensors in measuring displacement at a typical high-speed railroad bridge.

Keywords: displacement; railroad bridge; ring gauge; laser Doppler vibrometer; vision system; optoelectronic displacement meter

1. Introduction

Structural health monitoring (SHM) is a process to interpret status of a structure by analyzing collected responses from the structure. Since the responses are made by inputs given to the structure, SHM requires the information on the inputs that is hardly assessed on large civil structures. Thus, the modal properties (e.g., natural frequency, mode shape, and modal damping ratio) that are considered as unique features of a structure have widely been used for the SHM. However, the modal properties are ascertained to be insensitive to most types of structural changes and vulnerable to the environmental condition (Friswell and Penny 1997, Farrar and Jauregui 1998).

Recently, the paradigm of SHM technology is shifting from monitoring of the overall structure using a single type of response (e.g., acceleration) to monitoring of specific structural feature using responses with high sensitivity to the feature. The examples of the shifted paradigm are found here: bearing monitoring (Ha *et al.* 2011), cable tension (Cho *et al.* 2010, Sim *et al.* 2014), tendon monitoring (Kim *et al.* 2009, Xuan *et al.* 2009), concrete evaluation (Lim and Cao 2013, Hertlein 2013), reinforcement monitoring (Fernandes *et al.* 2013, Torres-Luque *et al.* 2014). The development of the specific monitoring techniques can be further lead to a composite monitoring using various types of responses to evaluate the performance of a structure.

∗Corresponding author, Associate Professor
 E-mail: ssim@unist.ac.kr
[a] Assistant Professor
[b] Ph.D. Student

For railroad bridges, deflection (i.e., vertical displacement) by passing trains is an important parameter that should be monitored to ensure the stability of railroads (Ni *et al.* 2010, Ni *et al.* 2012). In Korea, the design criteria specify the maximum deflection of railroad bridges to guarantee the comfort of passengers as well as the structural safety (MTLM 2011): L/2200 for comfort and L/600 for structural safety where L (m) is the span length. In addition, the maximum twist of rail is specified as 1.2 mm every 3 m. Therefore, the deflection measurement with sub-millimeter accuracy is essential to investigate whether a railroad bridge meets the design criteria or not.

Currently, many sensors (or sensing systems) have been developed to measure the displacement; the most famous are contact-type transducers such as the linear variable differential transformers (LVDT) and the ring gauges. They use an elastic part (e.g., a spring-ended rod or a wire) to be contacted to a structure and the deformation of the contacted part is recorded using the corresponding signal conditioner (Baumeister and Marks 2006, TML 2014). Laser Doppler vibrometers (LDV) are emerging due to its noncontact mechanism and high accuracy. The LDV measures velocity and displacement using the Doppler shift of laser light scattered back from a moving object. Nassif *et al.* (2005) used the LDV to measure the vertical deflection of the Doremus Avenue Bridge, and verified its performance by comparing the deflections measured by an LDV and an LVDT. Vision-based displacement measurement systems (VDMS) are now actively under development due to the fast development of inexpensive video devices and computer vision algorithms (Lee *et al.* 2006, Chang and Xiao 2010, Fukuda *et al.* 2013, Busca *et al.* 2014). The VDMS records the structural movement using a camera and interpret the displacement by tracking a

natural feature or an artificial marker on the structure. By locating the camera free of vibration and recording the movement with reasonable resolution, the VDMS provides dynamic displacement with sub-millimeter accuracy. Besides, there are many other sensors available in the market, such as optoelectric displacement meters (ODM), global positioning systems (GPS), and so on.

Despite of the availability of various sensors, displacement is currently being measured at most of large structures using the conventional contact-type sensors. This disproportionate usage of sensors seems to originate from conservation and inertia of civil engineering field; civil engineers tend to use sensors that have been previously validated from various fields and they do not like to use unfamiliar techniques. To encourage civil engineers to use various sensors according to their specific purposes and target structures, comparative study of the sensors can be effective to show the performances of the available sensors under the same environment. Furthermore, the explanation of additional features, such as cost, easiness, and robustness of the sensors, can help the civil engineers to select the most appropriate solution to their tasks related to the displacement measurement.

This paper presents a comparative study of displacement measurement using four sensors that are being used in the field: they are a ring gauge, a laser Doppler vibrometer (LDV), a vision-based displacement measurement system (VDMS), and an optoelectronic displacement meter (ODM). The comparative study was carried out on a brand-new high-speed railroad bridge. The bridge was designed to produce displacements within a couple of millimeters under the loading of a high-speed train, and thus, the measurements should keep precision of sub-millimeter to assess the status of the bridge accurately. The installation and measurement procedures for the four sensors are introduced to show their pros and cons, and the measured displacements are compared in the time and frequency domain to show the performances.

2. Sensors for displacement measurement

This section briefly introduces the working principles of the four sensors (or sensing systems) that are being mostly used in the field for displacement measurement. Note that the global positioning system (GPS), despite of its popularity, was not considered in this study due to its large resolution in the order of millimeters (Jo *et al.* 2013).

2.1 Ring gauge

The ring gauge is a contact-type displacement transducer that is most widely used for large civil structures (e.g., bridges). This transducer has a round plate spring where two strain gauges are attached as shown in Fig. 1. At the top of the plate spring, a probe can be mounted to be pressed against a structure. If the structure deforms, the probe deforms the plate spring and the strain change is measured as a voltage signal through a Wheatstone bridge. The ring gauge has a straightforward manner of operation

and high sensitivity, which is the reason why it is widely used in the field.

When the measured structure is not easily reachable, the ring gauge uses a fixed scaffold or an extended probe. A tensioned wire, shown in Fig. 2, is the most popular extended probe for bridges due to its cost-effectiveness and easy installation. The tensioned wire, however, may result in biased or contaminated measurement when the tension lacks or wind excites the wire.

It is worthy to note that the linear variable differential transformer (LVDT), the most famous displacement transducer due to its high sensitivity, repeatability and environmental durability, is not used in this study due to its limited applicability to the large structure. The LVDT requires a high scaffold to contact the measurement location at a large structure, which significantly increases the measurement cost. Meanwhile, the ring gauge can use a tensioned wire to contact the sensor to the measurement location, which saves the measurement cost while keeps the applicability at the large structures.

2.2 Laser Doppler Vibrometer (LDV)

The LDV system is a non-contact type system to measure the vibrations on a structural surface. The LDV provides both readings of velocity and displacement based on laser interferometry. The LDV is based on the detection of the Doppler shift of laser light when reflected back from a vibrating object (Nassif *et al.* 2005).
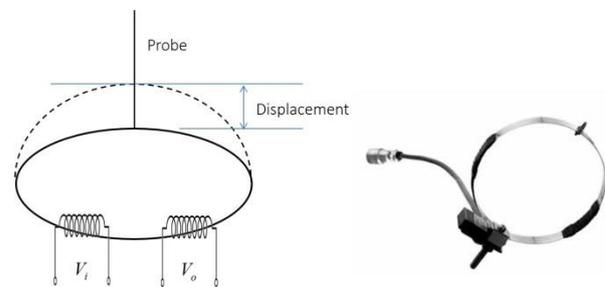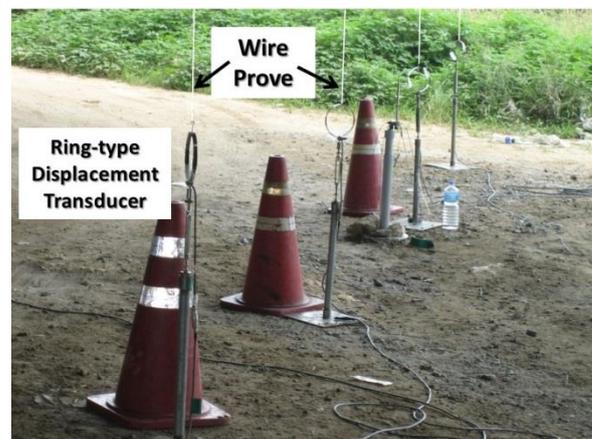

Fig. 1 Ring gauge (TML 2014)

Fig. 2 Field application of ring gauges using tensioned wire as an extended probe

An object moving away from the sensor head will reflect light that has a lower frequency, and vice versa. The LDV splits a laser beam into two: a reference beam and a test beam. The reference beam has a known frequency and phase, and a test beam is reflected back from the structure with Doppler shift. They are mixed together and pass through a two-beam laser interferometer that measures the frequency and phase difference between two beams. Then, the velocity and displacement d of the moving object can be obtained as

$$v = \lambda \Delta f / 2 \qquad (1)$$

$$d = \lambda \Delta \phi / 2 \qquad (2)$$

where λ is the wavelength of the light; and Δf and $\Delta \phi$ are the difference of frequency and phase between two beams, respectively. The schematic of the LDV is illustrated at Fig. 3.

The LDV is advantageous when the structure is hard to reach. The LDV can measure the displacement with micrometer resolution of a structure distant over 100m. Coinciding with the performance, the cost is very high for a single-point measurement. Though there is an LDV that can scan multiple points simultaneously, it is still under development for accurate measurement (Allen and Aguilar 2009).

2.3 Vision-based Displacement Measurement System (VDMS)

The VDMS is a novel system to use an imaging device as a sensor. The VDMS simulates the ocular sensing to measure displacement. After capturing the structural movement using the imaging device such as a camera, the movement in a series of images is converted into a physical movement by building a relationship between the image coordinate system (ICS) and the world coordinate system (WCS), which is the name of the physical coordinate system.

The VDMS used in this study is a monocular vision system that is developed upon the prototype proposed by Lee and Shinozuka (2006). The hardware of the system is composed of a CCD-based analog camera with optical zoom, a black marker with four white dots, a laptop computer to process the images, and a frame grabber to deliver the image from the camera to the laptop as shown in Fig. 4. A series of images of the marker are captured at the sampling rate supported by the camera. In general, 29.97fps (frame per second) or higher is supported by off-the-shelf cameras. In the system of Lee and Shinozuka, a kind of affine transform was used to build the relationship between the movement of white dots in the image and on the real marker. In the present system, a planar homography was used to consider the transform in the projective space where the images are obtained. The VDMS has been validated from in-lab and outdoor field applications (Lee and Shinozuka 2006, Lee *et al.* 2007, Lee *et al.* 2017).
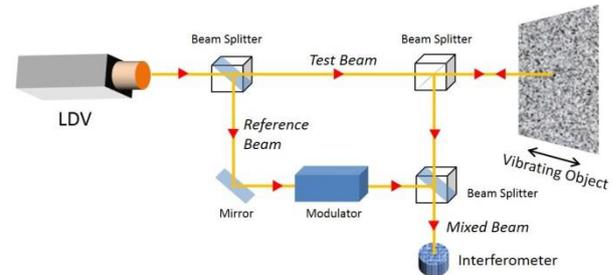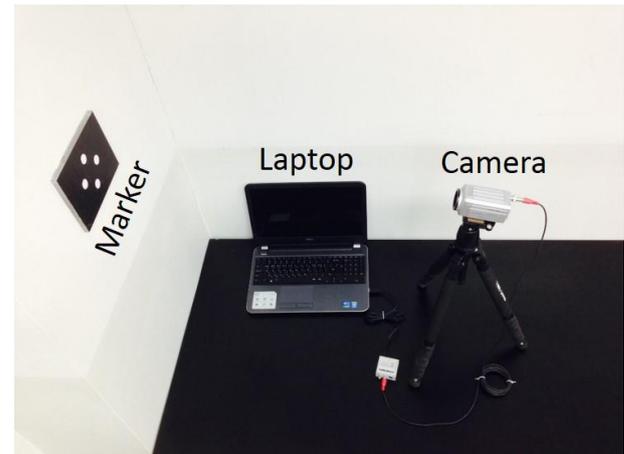

Fig. 3 Operating schematic of LDV

Fig. 4 Components of VDMS prototype

Though the system was shown to be effective for the measurement of small-scale displacement in the order of millimeters at large civil structures, the limited spatial resolution of imaging sensors may bring a significant error. For example, the CCD camera that generally has 0.3 megapixel has the spatial resolution of 640×480 pixels. If the target whose vertical length is 10 cm is in the field of view (FOV) of the camera, the pixel resolution (i.e., a displacement that can be captured by a pixel) for the vertical measurement is 100(mm)/480(pixel) = 0.21 mm, which may become larger due to larger target size and larger field of view. Though the pixel resolution can be reduced by employing subpixel algorithms (Wang *et al.* 2004), the pixel resolution still might not be enough for small-scale displacement measurement. Therefore, the pixel resolution needs to be optimized based on the test purpose and scale of measurement.

2.4 Optoelectronic Displacement Meter (ODM)

The ODM measures displacement of a target structure using time-of-flight (TOF) of light. Basically, the ODM is developed to measure the position of a structure. Displacement, equal to the change of positions, can be obtained from continuously measured positions of a structure. The ODM is generally composed of a light source, an optoelectronic receiver, and a retro-reflector. After attaching a reflector on the structure, the structure's position is continuously obtained by analyzing the TOF on the light path. A reflector or prism that returns the light to the receiver for TOF analysis is used as the reflector.

Table 1 Specifications of used sensors

Sensor	Model	Implemented Test	Specification
Ring gauge	TML OU-30	First/Second Tests	• Sampling rate = 500Hz • Frequency response = 20 Hz • Measurable range = 30 mm • Cost ≈ $3,000
LDV	Polytec RSV-150	First/Second Tests	• Sampling rate = 1200 Hz (Max. 2 MHz) • Resolution = 0.3 nm • Measurable distance ≥300 m • Cost ≈ $100,000
VDMS	Samsung SCZ-2373	First/Second Tests	• Sampling rate = 29.97 Hz • Optical zoom = ×37 (3.5 – 129.5 mm) • Effective pixels = 976(H) × 494(V) • Cost ≈ $1,000
ODM	Noptel PSM-R/M2	First Test	• Sampling rate = 200 Hz • Resolution = 0.2 mm at 20 m distance • Measurable range = 0.15 m at 20 m distance • Measurable distance = 20-400 m • Cost ≈ $15,000
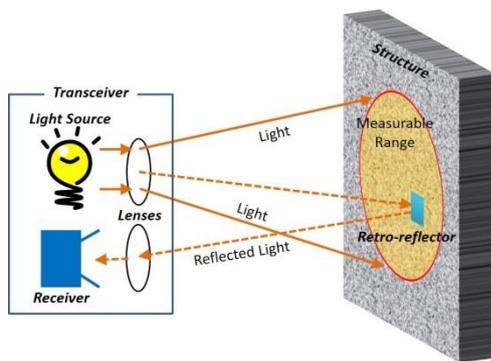
Fig. 5 Operating schematic of ODM

Fig. 6 Test bridge and measurement locations

Fig. 5 shows the operating schematic of the ODM. The light source shoots a light beam to the structure through a concave lens that spreads the light. The spread light forms measurable range of the ODM. A light beam heading to the retro-reflector attached on the structure is reflected to the receiver. Then, the TOF of the reflected light is calculated to measure the position of the reflector. The light source and receiver together is generally called as a transceiver.

3. Overview of measurement test

3.1 Test bridge

The comparative study of the four sensors was carried out on a high-speed railroad bridge. The test bridge is on the Honam train line rebuilt as a parallel track to run a high-speed train, so-called KTX (Korea Train eXpress). The test bridge, shown in Fig. 6, is a single-span steel plate girder bridge whose span length is 50 m. The bridge has two main plate girders (east and west) that support two directional rails (southbound and northbound).
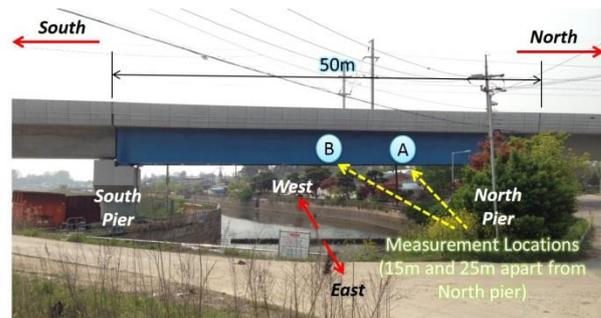
The comparative study was carried out as a part of validation for the new bridge after its construction. This new bridge required validation of safety and performance before opening the service for the KTX train to the public. Deflection was measured to check satisfaction of the railroad bridge design criteria of Korea (MTLM 2011). The design criteria limit the deflection at the center of the bridge to ensure the safety of rails and to prevent discomfort of passengers on the train.

Two times of tests were carried out with different sensor configurations and loading trains. In both tests, measurement was carried out at two locations of the west-side girder due to a rivulet under the bridge as shown in Fig. 6. The rivulet makes inaccessible the center of the bridge that is expected to have maximum deflection. Thus, the sensors that should be aligned with measurement direction (i.e., vertically) – a ring gauge, and LDV – were installed to measure Location A (15 m apart from the North pier), while the sensors whose performance is not significantly affected by their locations – VDMS and ODM – were installed to measure Location B (the center of the bridge). The detailed sensor configurations will be described in the subsequent section.

(a) Picture of installed sensors
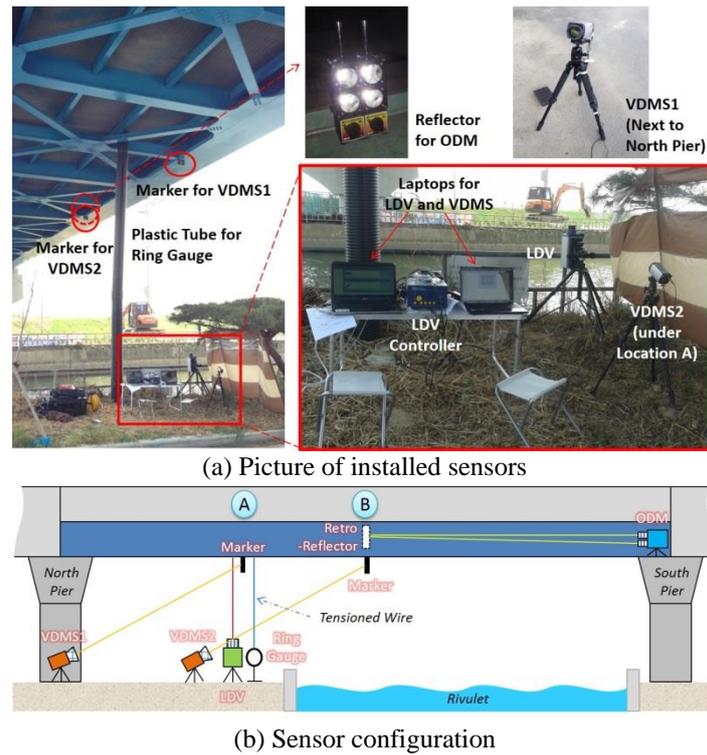

(b) Sensor configuration

Fig. 7 Sensors installed in the first test

3.2 Specifications of used sensors

The specifications of the sensors used in both tests are tabulated in Table 1. Looking only at the tabulated specifications, the LDV has the best performance in the resolution, sampling frequency, and measurable distance, while the cost is exorbitant. The ODM seems to have long measurable distance, appropriate sampling rate for civil structures, and reasonable cost. The VDMS has competitive cost but low sampling rate, while its performance highly depends on the used camera and lens. The ring gauge is inexpensive, but it has low frequency response that significantly limits dynamic measurement.

4. Displacement measurement on high-speed railroad bridge

4.1 First test

4.1.1 Test scenarios and setup

The first test was carried out with a KTX train that runs up to 300 km/h to load the bridge simulating the practical service. The train was composed of eight passenger cars and two heavy engines at both ends. The train ran 13 times with various speeds, headings (i.e., directions), and rails as tabulated in Table 2, and the speeds are obtained manually from the train odometer by a person on board.

In the first test, four types of sensors were implemented: a ring gauge, an LDV, two VDMSs, and an ODM. The measurement locations of the sensors were determined upon their flexibility of alignment: a ring gauge, an LDV, and a

Table 2 Running scenarios of train in the first test

Train	Scenario Name	Speed (km/h)	Heading	Rail
	K-1	60	South	East
	K-2	230	North	East
	K-3	270	South	East
	K-4	270	North	East
	K-5	230	South	West
	K-6	230	North	West
KTX	K-7	270	South	West
	K-8	270	North	West
	K-9	60	South	East
	K-10	270	North	East
	K-11	300	South	East
	K-12	300	North	East
	K-13	300	South	West

VDMS (i.e., VDMS1) was used to measure Location A, while the other VDMS (i.e., VDMS2) and an ODM was used to measure Location B. The ring gauge used a tensioned wire as an extended probe, which was covered by a plastic tube to eliminate the perturbation by wind. The LDV was installed under the Location A. The VDMS1 and VDMS2 were installed at the locations about 17 m and 15 m apart from the measurement locations, respectively. The reflector of the ODM was installed on the west girder of Location B, while the transmitter of the ODM was installed
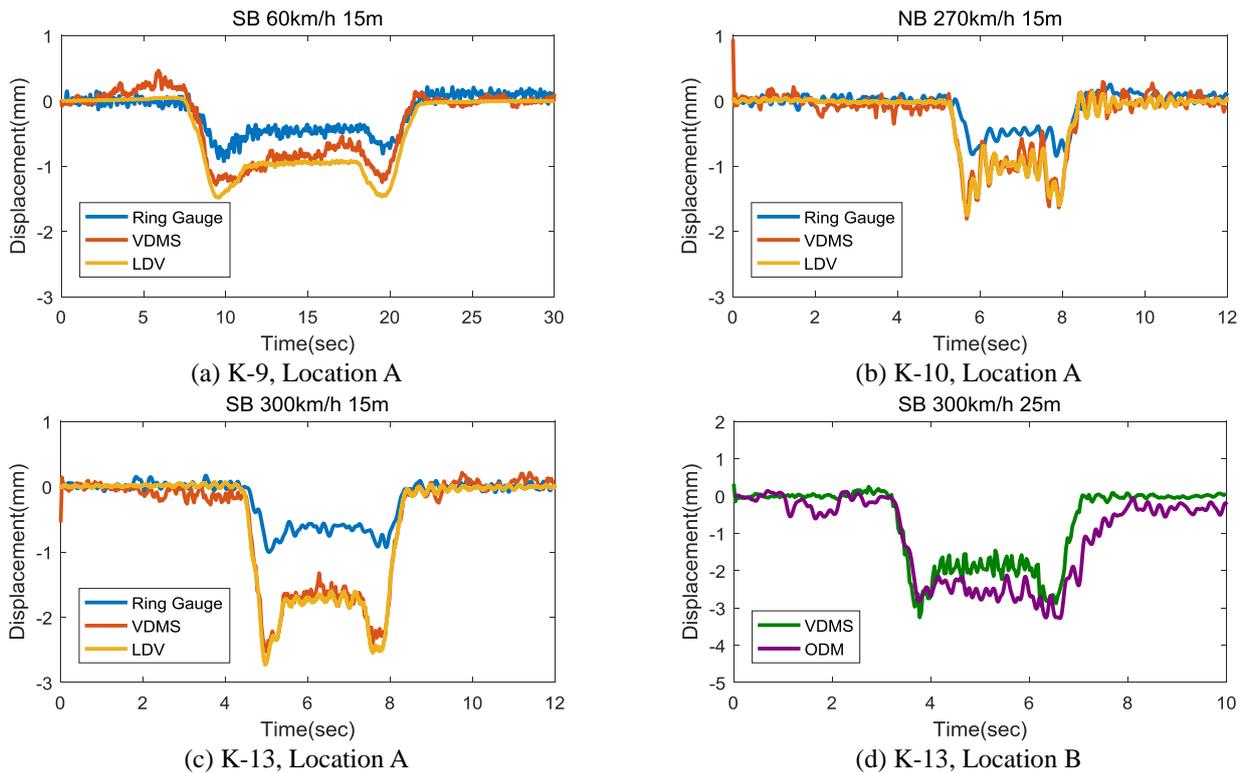
Fig. 8 Four examples of measured displacements in the first test

4.1.2 Displacement measured in the first test

The displacements for 13 KTX running Scenarios were measured, and Fig. 8 shows four selected examples. (All the displacements measured in the first test can be referred to the appendix of this paper.) Note that the displacements measured using independent measurement systems were synchronized in the time domain by calculation of maximum cross correlation overall, the measured displacements are in the order of millimeters, and they show W-shape with two peaks at the start and end due to two heavy engines of KTX train at both ends. When the train runs faster than 100 km/h, the dynamic fluctuations excited by a series of connected cars are also observed between two peaks as shown in Figs. 8(b)-8(d). The displacement at Location B is slightly larger than that at Location A, as compared in Figs. 8(c) and 8(d). All the measured displacement shows that the four sensors used in this study are capable of measuring displacement of the high-speed railroad bridge, though their performance is different. Regardless of the rail the train ran on, the ring gauge resulted in similar level of displacements (around 1 mm at the first peak) while the others show varying levels. Since the ring gauge still shows W-shape displacement, the cause of the small displacement is presumed to be poor installation of the tensioned wire in the field. The tensioned wire might get loose or touch the plastic tube shown in Fig.

7(a), which could not exactly be observed due to the opaque plastic tube. The noise caused by the poor installation of the extended probe is the well-known drawback of the contact-type gauges including ring gauges and LVDTs.

4.2 Second test

4.2.1 Test scenarios and setup

The second test was carried out four months after the first test. In the second test, a HEMU (Highspeed Electric Multiple Unit) train that runs up to 400 km/h was employed to load the bridge. The HEMU was composed of six passenger cars with distributed traction, and thus the excitation trend is different from that of the KTX train used in the first test. In the second test, the HEMU train ran four times with the running scenario tabulated in Table 3.

The goals of the second test are validation of the new bridge safety under the different excitation condition by a HEMU train and additional validation of sensors. Since the ring gauge resulted in poor performance in the first test due to the windy environment, the second test was carried out using three sensors to measure Location A as shown in Fig. 9: a ring gauge, a LDV, and a VDMS. To avoid the mistake in the first test made possibly by the tensioned wire, a steel bar whose end is connected to a plate is used instead as an extended probe for the ring gauge. One VDMS was installed about 17 m apart from Location A where the marker was installed, similar to the first test.
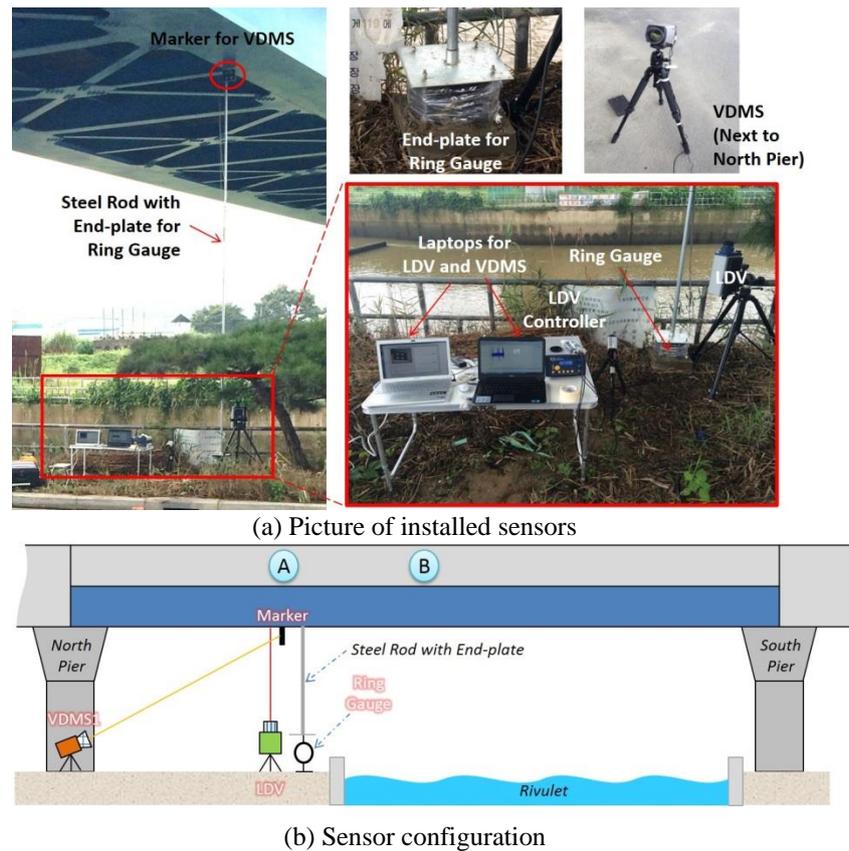
(a) Picture of installed sensors

(b) Sensor configuration

Fig. 9 Sensors installed in the second test

Table 3 Running scenarios of train in thesecond test

Test	Scenario Name	Train	Speed (km/h)	Heading	Rail
Second Test	H-1	HEMU	210	South	West
	H-2		250	North	West
	H-3		210	South	West
	H-4		250	North	West

4.2.2 Displacement measured in the second test

The displacements for four HEMU running Scenarios were measured, and Fig. 10 shows the measured displacement. Different from W-shape displacement made by a KTX train led by two heavy engines at both ends, the displacement measured in the second test shows nearly equal six fluctuations made by the six cars with distributed traction. In the second test, the ring gauge measured comparative displacement with the other displacement due to the wind-resistive steel rod. All sensors successfully captured dynamic patterns even in the residual vibration, though there are small differences in the amplitude.

4.3 Comparison of measured displacement

The detailed comparison of the displacements measured by four sensors is given in this section. The comparison is made on the measurement noise, peak displacement, and frequency response.

4.3.1 Measurement noise

The measurement noise originates from various reasons: inherent noise from the sensor system, vulnerability to the external loading, weakness of measurement accessories, and sensitivity to the environmental condition.The measurement noise level of the used sensors is investigated here by looking at several measurement examples.

The LDV measures the displacement with the highest accuracy when investigated visually. As shown in Figs. 10 and 11, the LDV accurately measured displacements with clear patterns according to the train type, changing amplitudes according to the train scenarios, and dynamic fluctuations between two peaks. The apparent noise level is very low, and zero displacements were stably measured before and after the train passing. The only shortcoming of the LDV was the installation point; the LDV has to shoot the light in the measurement direction and could not be installed to measure Location B due to the rivulet. If the LDV is installed with angle to the measurement point, then laser is not fully reflected to the LDV and the LDV shows significant noise.

Though the VDMS shows considerable accuracy in the Figs. 10 and 11, the VDMS measured two typical noises: (1) by the camera vibration and (2) by high illumination.

The first type of noise is observed in the middle of excitation at K1-K3, and before and after the excitation in most of the Scenarios. The serious noise shown in Fig. 11(a) was from camera vibration by the passing train.
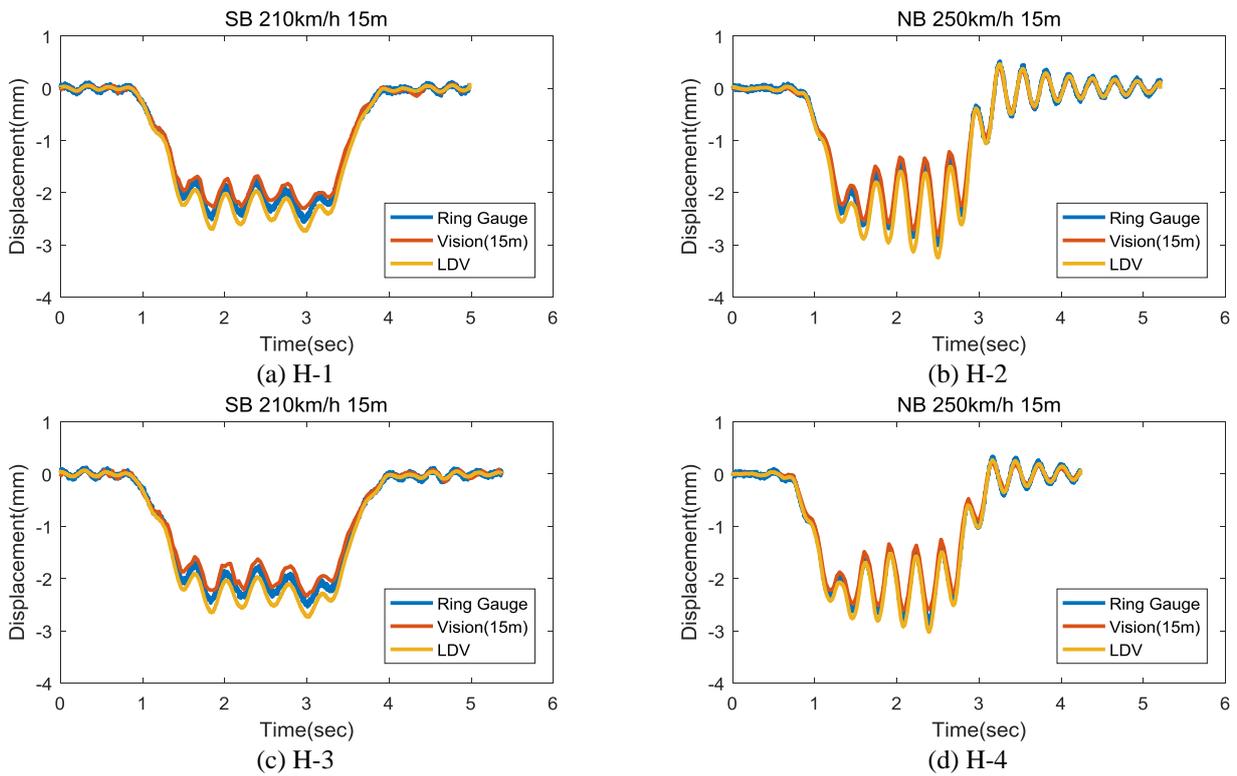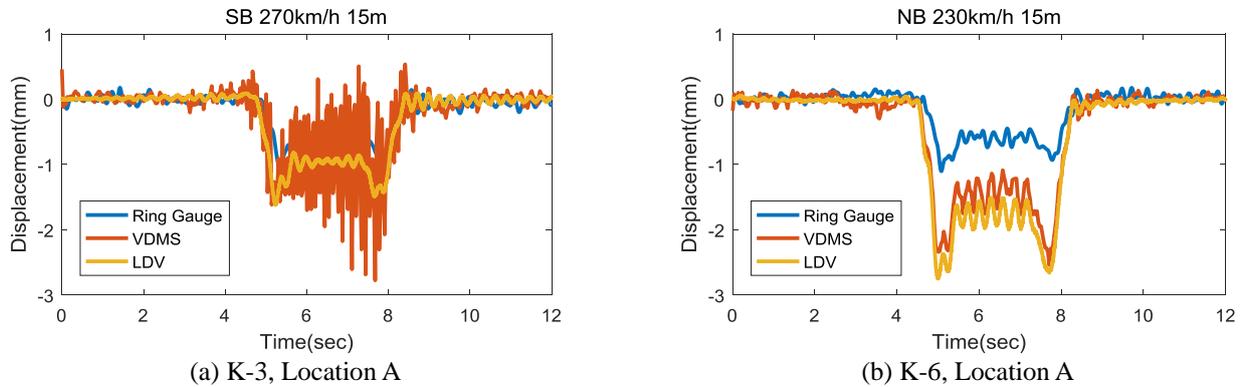
Fig. 10 Measured displacements in the second test

Fig. 11 Two typical measurement noise of VDMS by camera vibration and high illumination

In the initial test setup, the camera was installed next to a bridge pier, which brought serious vibration by the passing train as the ODM did. After K3, the camera was moved distant to the pier to avoid the train vibration and the serious noise was not observed any more. The noises observed before and after the excitation originate from wind vibration. The telescopic lens significantly amplifies small vibration of the camera excited by the wind, and thus stable pose of the camera must be secured by blocking the wind. The second type of noise is observed in the middle of excitation at K6, K9, K11 and K12. High illumination outdoors may make unbalanced light on the marker and hinders accurate search of feature all Scenarios.

The ODM measured displacements with high level of noises that destroy the W-shape patterns for most of the Scenarios as shown in Fig. 13, which also results in inaccurate peak displacements. The high noises resulted from the vibration of transmitter installed on the south pier of the bridge. Fig. 13 shows two examples of bad measurement by the ODM. Especially, jerks due to the transmitter vibration appear before the first peak for NB trains and after the first peak for SB trains, respectively. Since the piers were the only position to shoot a light to the retro-reflector at the measurement location, the noise created by the train vibration is hard to be removed in the measurement.

(a) Low illumination

(b) High illumination
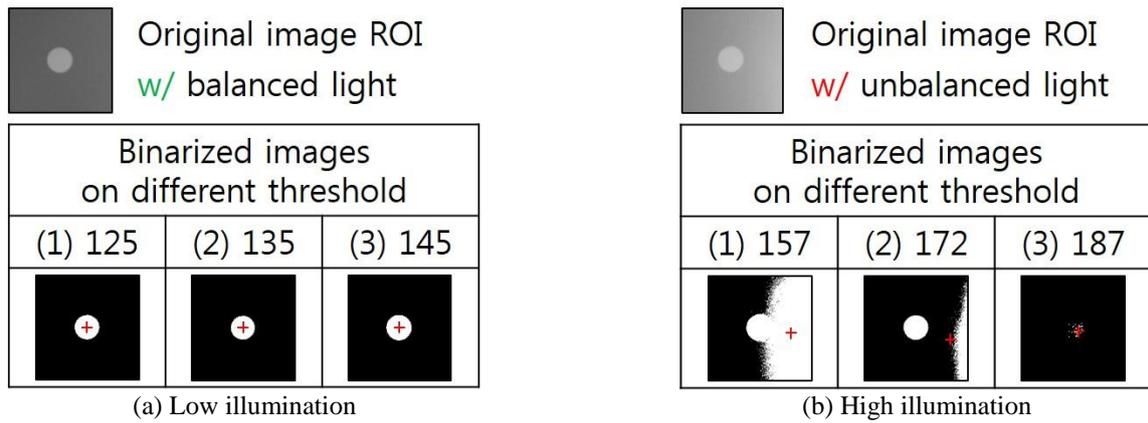
Fig. 12 Feature location (red-cross mark) found by binarization in different light conditions

(a) K-2, Location B

(b) K-3, Location B

Fig. 13 Examples of bad measurement by the ODM
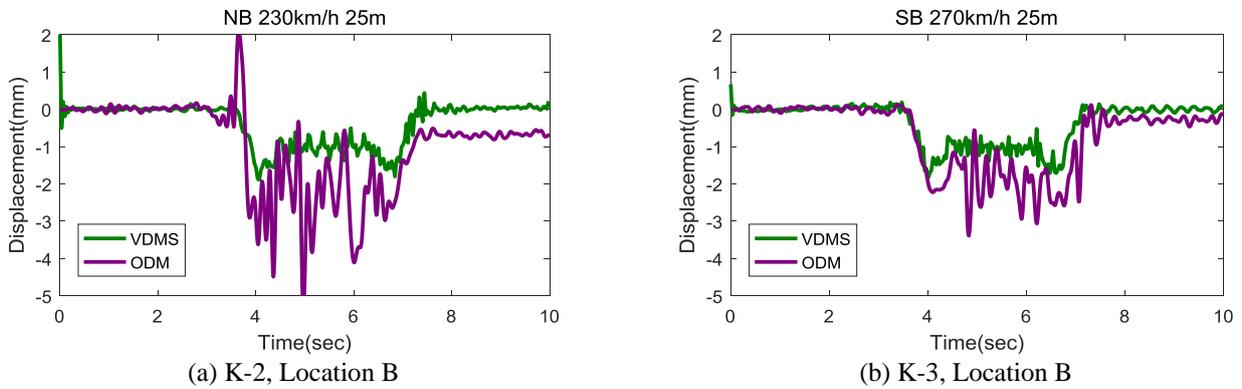
(a) Left peak displacement
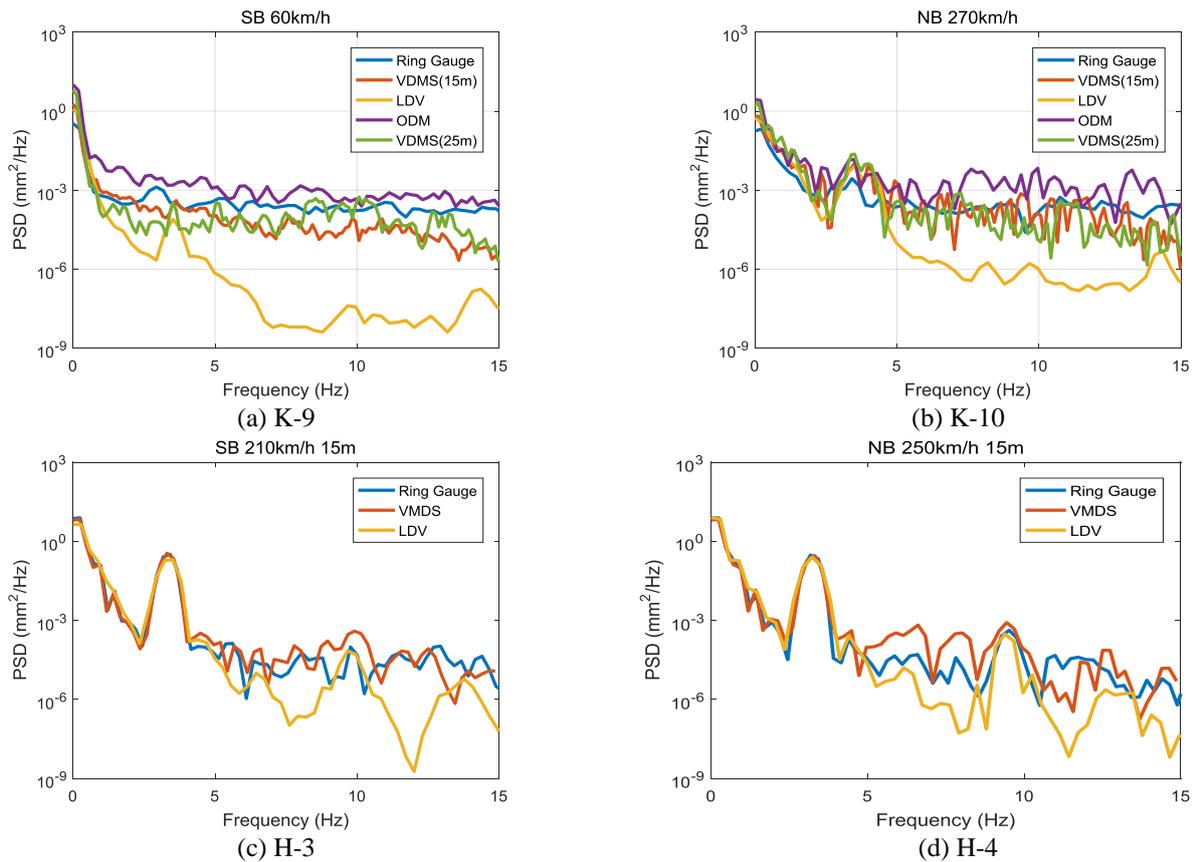

(b) Right peak displacement
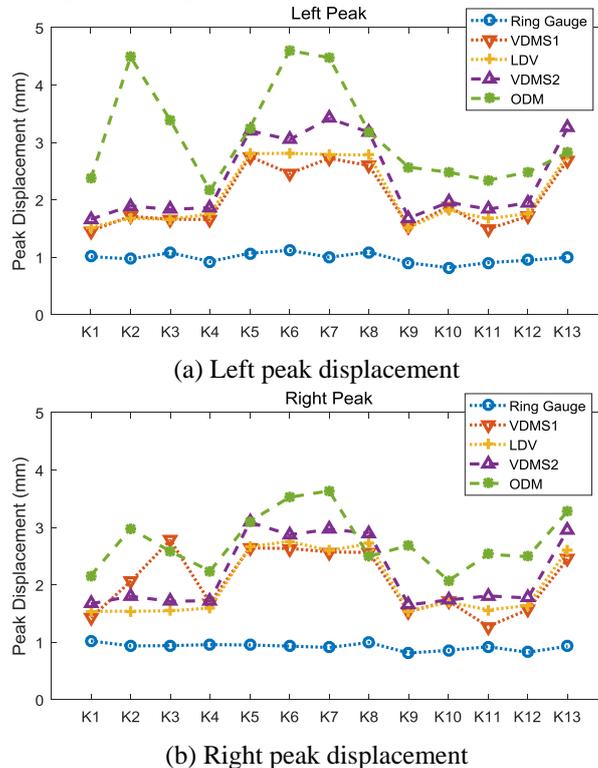
Fig. 14 Peak displacement of first test

Fig. 15 Power spectral density of measured displacements

4.3.2 Peak displacement

The peak displacement is the maximum displacement excited by the train loading, and it is one of the most important measurement when validating a newly built railroad bridge. However, when the train is running with very high speed, the peak displacement may not be captured exactly due to insufficient sampling frequency and measurement noise.

Fig. 14 shows peak displacement of 13 Scenarios in the first test. Since the displacement is W-shape with two peaks, left and right peak displacements are separately plotted. Since the sensors are installed at the west side of the girder, Scenarios with train on the west rail show large displacement than the others. LDV could measure very consistent values: about 1.5 mm for Scenarios with the train running slow on the east rail (e.g., K1 and K9), 1.6-1.8 mm for Scenarios with the train running fast on the east rail (e.g., K2-K4 and K10-K12), and 2.6-2.8 mm for Scenarios with train running fast on the west rail (e.g., K5-K8 and K13). Two VDMS captured the peak displacement with good accuracy. The VDMS2 of Location B provides larger peak values than VDMS1 of Location A substantially. Variation of peak displacements in similar Scenarios, which is not shown in the graphs of the LDV, and large right peak displacements at K2 and K3 shown in Fig. 14(b) is due to measurement noise described earlier. The ODM measured inaccurate peak displacement due to high level of noise and jerks caused by the inevitable installation of transmitter on

the pier. The ring gauge shows almost consistent level of displacement due to possible poor installation of the tensioned wire.

4.3.3 Frequency response

Fig. 15 is the power spectral density (PSD) of displacements in K9 and K10 in the first test and H3 and H4 in the second test. The noise levels are observed in the frequency domain. The noise level is high in the sequence of ODM, ring gauge, VDMS, and LDV in the first test, and in the sequence of VDMS, ring gauge, and LDV in the second test. The lowest noise level of the LDV is noticeable. Even with the short measurement of 10 seconds, the LDV could clearly capture the peak around 3 Hz which is the first natural frequency of the test bridge in both tests. The low noise level of LDV shows some peaks in higher frequencies that may be from the dynamic fluctuations by cars. In the second test, all used sensors (VDMS, ring gauge, VDMS, and LDV) could capture the peak very clearly due good excitation of HEMU.

However, due to high level of noise observed even in low frequencies, the ring gauge, VDMS, and ODM failed to get informative values in higher frequencies than 15 Hz, which is the maximum frequency range in Fig. 15. The ring gauge even could capture the second peak around 9 Hz when used with a steel rod which is sometimes hard to install at high bridges. The VDMS has the noise level on edge of success and failure to capture the first peak in the

first test and the second peak in the second test. The ODM showed highest level of noise and is the only sensor that missed the first peak that could be captured by the other sensors as shown in Fig. 15(b). Recall that the high noise level of the ODM and the ring gauge comes from the train vibration and the poor installation of the tensioned wire.

5. Conclusions

This paper compared the displacement measured at a high-speed railroad bridge using four different sensors that are widely used in the field: a ring gauge, a laser Doppler vibrometer, a vision-based displacement measurement system, and an optoelectronic displacement meter. The measurement tests were carried out on a single-span steel plate girder bridge, which was newly built with the span length of 50m. Two times of tests were carried out with different train loadings: KTX and HEMU. The relative performance is presented by comparing the specification. The comparison can be summarized as:

(1) The LDV shows the best performance in the accuracy with little measurement noise in both tests, though its cost is exorbitant. By looking at the displacement in the frequency domain, the LDV shows lowest level of noise and shows peaky responses in the high frequency range.

(2) The ring gauge failed in measuring the displacement in the first test due to loosening of tensioned wire which is used as an extended probe. In the second test using a steel rod as a probe, the ring gauge showed comparable measurement in the time and frequency domain. The ring gauge requires great care during installation when using a tensioned wire.

(3) The ODM showed highest level of noise due to the reflector on the pier that shook when the train crossed the bridge. The limited position of the reflector hinders accurate measurement when an undisturbed position is not secured. Due to the noise, the ODM was the only sensor that missed the first peak captured by all the other sensors.

(4) The VDMS showed good performance in measuring the displacement with inexpensive cost and little installation effort. Due to noncontact and free positioning of the camera, the VDMS could accurately measure the displacement at the center of the bridge under where could not be measured by the other sensors due to the rivulet. However, ambient vibration and high illumination around the camera causes significant measurement error due to the use of telescopic lens.

Acknowledgments

References

Allen, M.S. and Aguilar, D.M. (2009), "Model validation of a bolted beam using spatially detailed mode shapes measured by continuous-scan laser Doppler vibrometry", *Proceedings of the 50th AIAA/ASME/ASCE/AHS/ASC Structures, Structural Dynamics, and Materials Conference*, Palm Springs, California, USA.

Baumeister, T. and Marks, L.S. (2006), *Standard Handbook for Mechanical Engineers, (11th Ed.)*, McGraw-Hill, New York.

Busca, G., Cigada, A., Mazzoleni, P. and Zappa, E. (2014), "Vibration monitoring of multiple bridge points by means of a unique vision-based measuring system", *Exp. Mech.*, **54**, 255-271.

Chang, C.C. and Xiao, X.H. (2010), "Three-dimensional structural translation and rotation measurement using monocular videogrammetry", *J. Eng, Mech. -ASCE*, **136**(7), 840-848.

Cho, S., Lynch, J.P., Lee, J.J. and Yun, C.B. (2010), "Development of an automated wireless tension force estimation system for cable-stayed bridges", *J. Intel. Mat. Syst. Str.*, **21**(1), 361-375.

Farrar, C.R. and Jauregui, D.A. (1998), "Comparative study of damage identification algorithms applied to a bridge: I. Experiment", *Smart Mater. Struct.*, **7**(5), 704.

Fernandes, B., Titus, M., Nims, D.K., Ghorbanpoor, A. and Devabhaktuni, V.K. (2013), "Practical assessment of magnetic methods for corrosion detection in an adjacent precast, prestressed concrete box-beam bridge", *Nondestruct. Test. Eval.*, **28**(2), 99-118.

Friswell, M.I. and Penny, J.E.T. (1997), "Is damage location using vibration measurements practical", EUROMECH 365 International Workshop: DAMAS (Vol. 97).

Fukuda, Y., Feng, M.Q., Narita, Y., Kaneko, S. and Tanaka, T. (2013), "Vision-based displacement sensor for monitoring dynamic response using robust object search algorithm", *IEEE Sens. J.*, **13**(12), 4725-4732.

Ha, D.H., Kim, D., Choo, J.F. and Goo, N.S. (2011), "Energy harvesting and monitoring using bridge bearing with built-in piezoelectric material", *Proceedings of the 7th International Conference on Networked Computing (INC)*, IEEE, Gumi, South Korea, 129-132.

Hertlein, B.H. (2013), "Stress wave testing of concrete: A 25-year review and a peek into the future", *Const. Build. Mat.*, **38**, 1240-1245.

Jo. H., Sim, S.H., Tatkowski, A., Spencer, Jr., B.F. and Nelson, M.E. (2013), "Feasibility of displacement monitoring using low-cost GPS receivers", *Struct. Control Health.*, **20**(9), 1240-1254.

Kim, J.T., Park, J.H., Hong, D.S., Cho, H.M., Na, W.B. and Yi, J.H. (2009), "Vibration and impedance monitoring for prestress-loss prediction in PSC girder bridges", *Smart Struct. Syst.*, **5**(1), 81-94.

Lee J-J. and Shinozuka, M. (2006), "A vision-based system for remote sensing of bridge displacement", *NDT & E Int.*, **39**(5), 425-431.

Lee, J., Lee, K.C., Cho, S. and Sim, S.H. (2017), "Computer vision-based structural displacement measurement robust to light-induced image degradation for in-service bridges", *Sensors*, **17**(10), 2317.

Lee, J.J., Fukuda, Y., Shinozuka, M., Cho, S. and Yun, C.B. (2007), "Development and application of a vision-based displacement measurement system for structural health monitoring of civil structures", *Smart Struct. Syst.*, **3**(3), 373-384.

Lim, M.K. and Cao, H. (2013), "Combining multiple NDT methods to improve testing effectiveness", *Constr. Build. Mater.*, **38**, 1310-1315.

Nassif, H.H., Gindy, M. and Davis, J. (2005), "Comparison of laser Doppler vibrometer with contact sensors for monitoring bridge deflection and vibration", *NDT & E Int.*, **38**(3), 213-218.

Ni, Y.Q., Ye, X.W. and Ko, J.M. (2010), "Monitoring-based fatigue reliability assessment of steel bridges: analytical model and application", *J. Struct. Eng. -ASCE*, **136**(12), 1563-1573.

Ni, Y.Q., Ye, X.W. and Ko, J.M. (2012), "Modeling of stress spectrum using long-term monitoring data and finite mixture distributions", *J. Eng. Mech. -ASCE*, **138**(2), 175-183.

Railway Design Standard (2011), Ministry of Land, Transport and Maritime Affairs (MLTM), 8-83 ~ 8-89.

Sim, S.H., Li, J., Jo, H., Park, J.W., Cho, S., Spencer, Jr., B.F. and Jung, H.J. (2014), "A wireless smart sensor network for automated monitoring of cable tension", *Smart Mater. Struct.*, **23**(2), 025006 (10pp).

TML   (2017), http://www.tml.jp/e/product/transducers/general/displacement/ou.html, Available at November 2017.

Torres-Luque, M., Bastidas-Arteaga, E., Schoefs, F., Sánchez-Silva, M. and Osma, J.F. (2014), "Non-destructive methods for measuring chloride ingress into concrete: State-of-the-art and future challenges", *Constr. Build. Mater.*, **68**, 68-81.

Wang, X., Gao, J. and Wang, L. (2004), "A survey of subpixel object localization for image measurement", *International Conference on Information Acquisition,* IEEE, 398-401.

Xuan, F.Z., Tang, H. and Tu, S.T. (2009), "In situ monitoring on prestress losses in the reinforced structure with fiber-optic sensors", *Measurement*, **42**(1), 107-111.
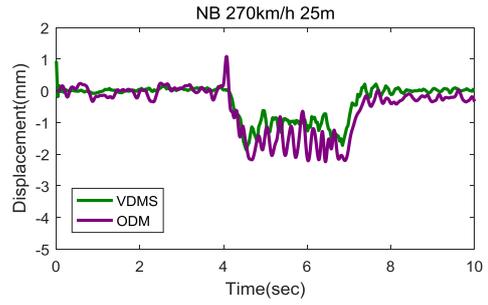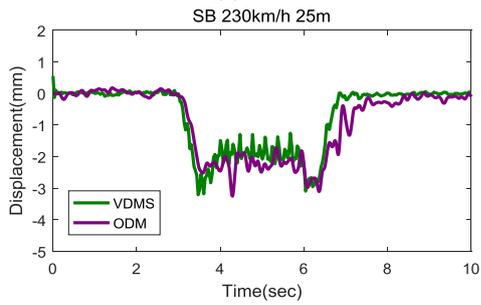
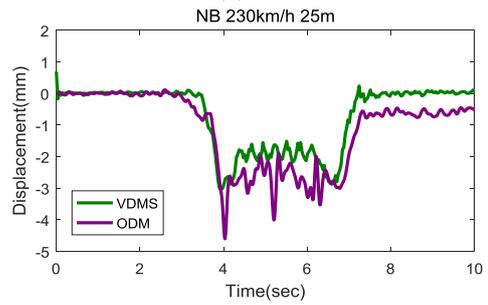## Appendix

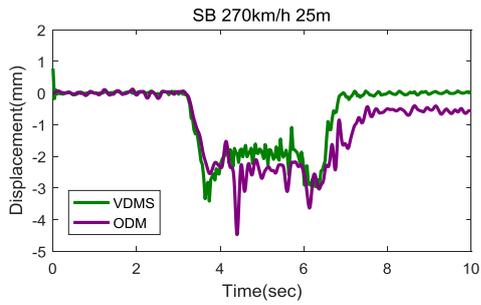Displacement measured in the first test.

(a) K-1

(b) K-2

(c) K-3
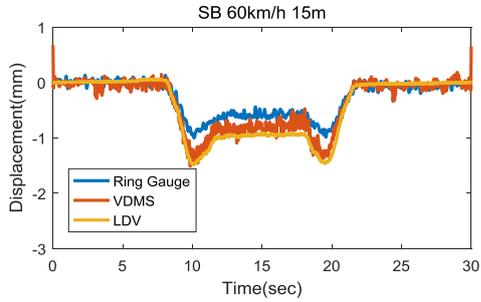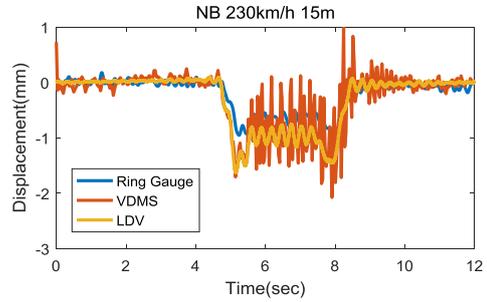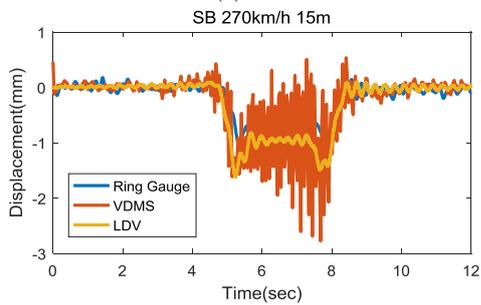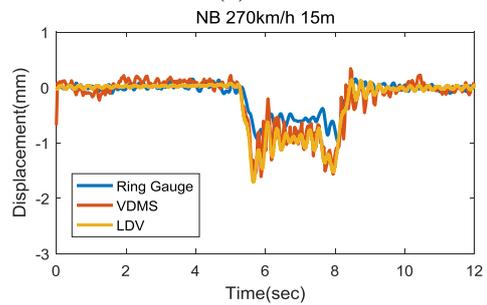
(d) K-4
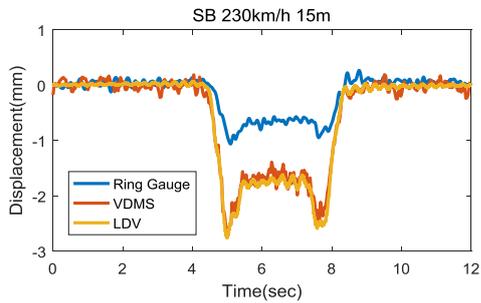
(e) K-5
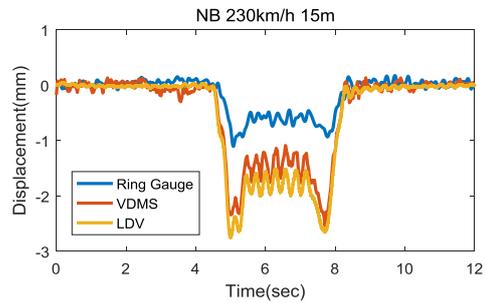
(f) K-6

(g) K-7

(h) K-8

Continued-

(i) K-9
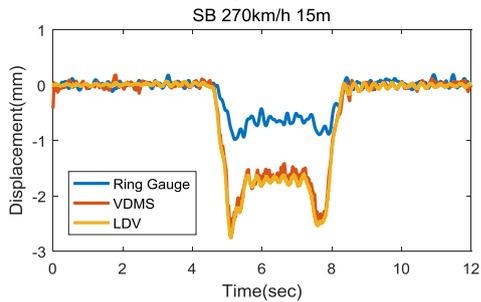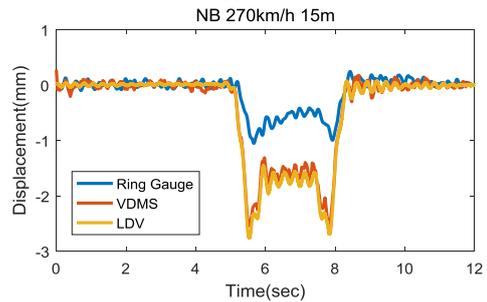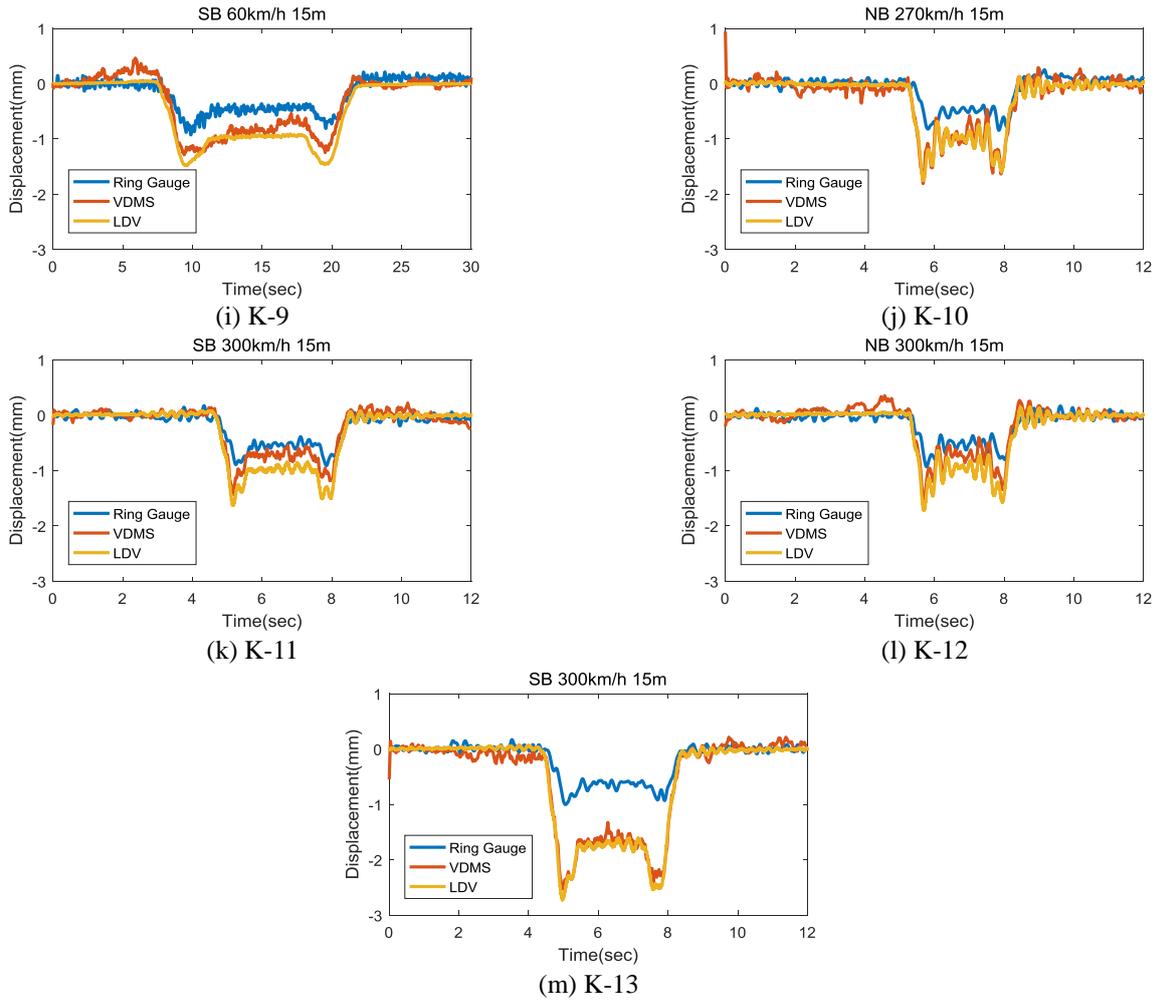
(j) K-10

(k) K-11

(l) K-12

(m) K-13

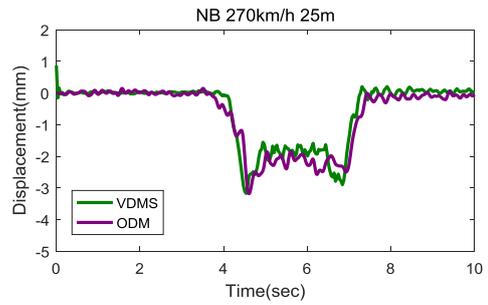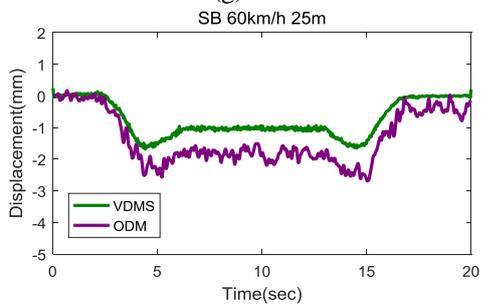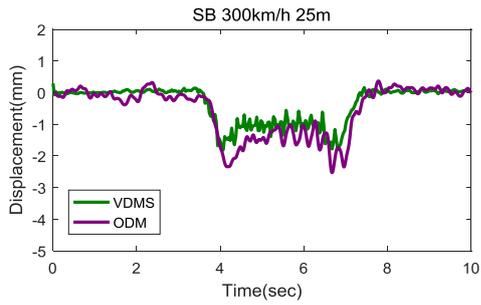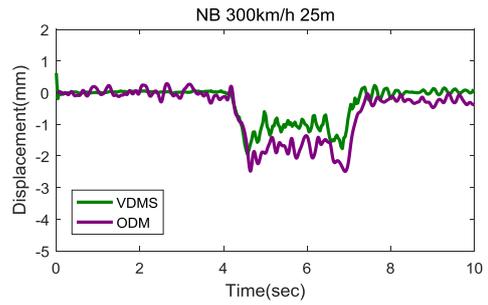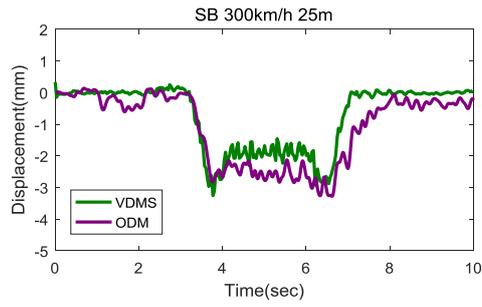Fig. A Displacement measured at Location A in the first test

(a) K-1

(b) K-2

(c) K-3
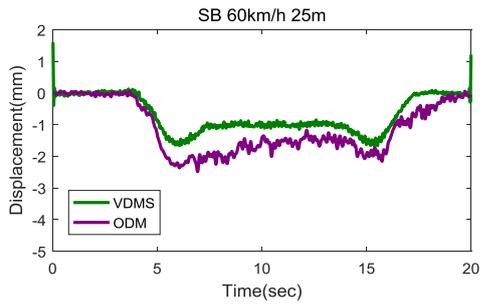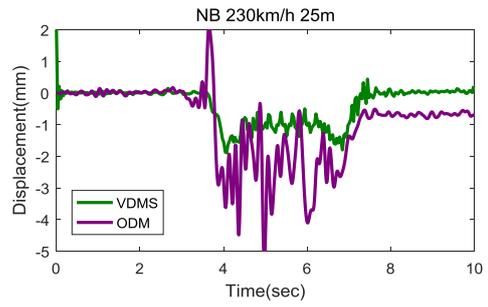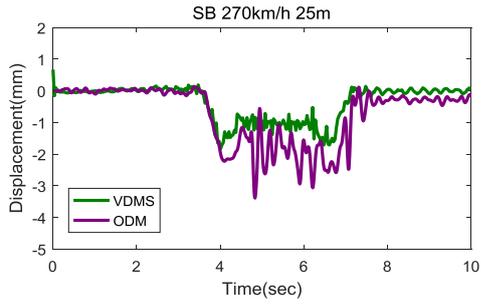
(d) K-4

(e) K-5

(f) K-6

(g) K-7

(h) K-8

(i) K-9

(j) K-10

Continued-

Soojin Cho, Junhwa Lee and Sung-Han Sim

SB 300km/h 25m

(k) K-11

NB 300km/h 25m

(l) K-12

SB 300km/h 25m
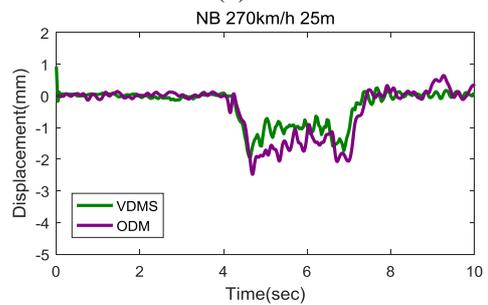
(m) K-13

Fig. B Displacement measured at Location B in the first test